

On-Site Transceiver Calibration via Constrained Adaptive Multi-layer Filters with Separating Tx/Rx Frequency Responses

Masaki Sato⁽¹⁾, Manabu Arikawa⁽¹⁾, Hidemi Noguchi⁽¹⁾, Junichiro Matsui⁽²⁾, Jun'ichi Abe⁽¹⁾
and Emmanuel Le Taillandier de Gabory⁽¹⁾

⁽¹⁾ Advanced Network Research Laboratories, NEC Corporation, 1753 Shimonumabe, Nakahara-Ku, Kawasaki, Kanagawa 211-8666, Japan, m-satou-kj@nec.com

⁽²⁾ NEC Corporation, 1131 Hinode, Abiko, Chiba 270-1198, Japan

Abstract We demonstrated transceiver calibration for 96-GBaud PM-64QAM via constrained adaptive multi-layer filters using weak Tx nonlinearity over 120 km SMF. By separating Tx/Rx frequency-dependent distortion, we showed flat Tx signal spectrum and 48 % reduction of 2x2 MIMO filter tap, compared to the conventional calibration. ©2023 The Author(s)

Introduction

Digital coherent transmission with higher symbol rate and higher-order modulation is essential to the accelerating global traffic demands [1]. As the symbol rate and modulation order increase, the signal-quality impact of frequency-dependent transceiver distortion becomes more significant. Coherent digital signal processor (DSP) typically has frequency domain equalizers (FDE) in the transmitter (Tx) and receiver (Rx) for Nyquist filtering and chromatic dispersion compensation (CDC). FDE is also used for the transceiver distortion compensation, including IQ crosstalk, and the filter coefficients of FDE are calibrated in the factory with dedicated hardware [2-4]. However, static calibration is not sufficient as these distortions are changing slowly with the temperature and aging of the devices. Adaptive equalization is being used to solve this issue [5-13] but at the cost of ASIC circuit resources.

An alternative consists in updating the filter coefficients of Tx and Rx FDE according to the situation when required using on-site calibration. Compensating for the corresponding distortion in the respective FDEs for Tx and Rx is preferable for resource-efficient implementation. A joint adaptive equalization scheme for both Tx and Rx impairment at the Rx DSP [9-13] can be used to derive the filter coefficients. In this field, a multi-layer (ML) filter architecture to compensate Tx/Rx impairment and polarization mode dispersion (PMD) has been proposed [9-11]. While several IQ imbalance estimations have been validated [10], the estimation for frequency-dependent distortion has not been studied so far.

To separate Tx/Rx distortion is not apparent as the common distortion of I and Q tributaries is

commutative. Thus, Tx and Rx IQ common distortions are interchangeable, making the estimation of the Tx and Rx distortions from ML filters difficult. Further, 2x2 strictly linear (SL) filter of ML filters for polarization demultiplexing also compensates for IQ common distortions, making Tx-Rx separation even more challenging.

In this paper, we propose on-site transceiver calibration with Tx-Rx separation using adaptive ML filters with polarization demultiplexing constraint (PDC) and weak Tx nonlinearity aid. The proposed method enables Tx-Rx separation and compensation of IQ common distortion, allowing precise calibration of Tx and Rx FDE in the main DSP without dedicated calibration hardware. Further, this calibration allows the main DSP to reduce the 2x2 SL filter taps, taking advantage of the FDE resource. We experimentally demonstrate our scheme with 96-GBaud Polarization Multiplexing-64 quadrature amplitude modulation (PM-64QAM) 120 km single mode fibre (SMF) transmission, effectively separating Tx/Rx frequency-dependent distortion. Compared to conventional calibration, we showed flat Tx frequency response within ± 0.8 dB ripple and 48 % reduction of 2x2 SL filter tap.

On-site transceiver calibration with Tx-Rx separation using adaptive multi-layer filters with PDC and weak Tx nonlinearity aid

The proposed transceiver calibration is based on ML filters to derive the filter coefficient of Tx and Rx FDE in the main DSP; it combines two schemes to realize Tx-Rx separation, including IQ common distortion. First, the concept of separating IQ common distortion in the fibre transmission system is depicted in Fig. 1. In the

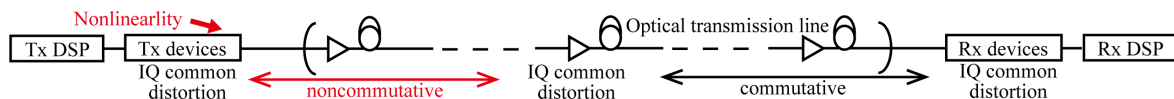


Fig. 1: Concept of separating IQ common distortion in the fibre transmission system

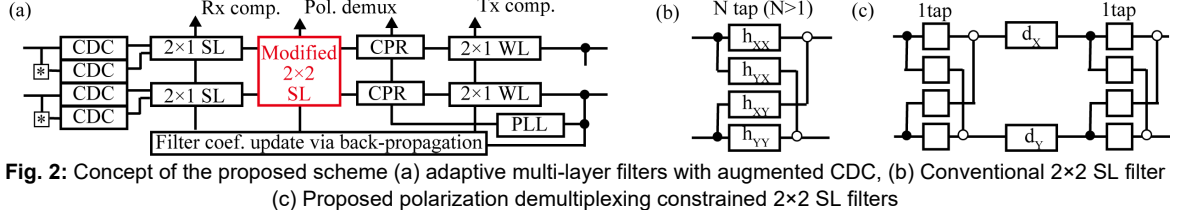


Fig. 2: Concept of the proposed scheme (a) adaptive multi-layer filters with augmented CDC, (b) Conventional 2×2 SL filter (c) Proposed polarization demultiplexing constrained 2×2 SL filters

linear region, each IQ common distortion of Tx, transmission line, and Rx is commutative, so it is difficult to separate each distortion. Nonlinear distortion makes this common distortion noncommutative. We take advantage of the operation at the beginning of the nonlinear regime at Tx device to make Tx-Rx separation.

Second, we modify ML filters with augmented CDC [11] in Fig. 2 (a) to derive the filter coefficients of Tx and Rx FDE in the main DSP. ML filters with augmented CDC consists of SL and widely linear (WL) filter layers, and the filter coefficients are adaptively controlled via back-propagation from the last outputs. CDC is performed on the received signal and its complex conjugate before ML filters. ML filters consist of Rx compensation, polarization demultiplexing by 2×2 SL filter, carrier phase recovery (CPR), and Tx compensation.

Generally, the 2×2 SL filter requires multiple taps to compensate PMD described in Fig. 2 (b); it also equalizes IQ common distortion in Tx and Rx. Although single tap avoids this phenomenon, it is not applicable since a small amount of PMD is always present in components like EDFA. The polarization behavior on the transmission can be modeled with polarization rotation and delay between polarizations [14]. Based on this, the multi-tap 2×2 SL filter can be transformed, as shown in Fig. 2 (c). The inter-polarization delay d_x and d_y are compensated by a single-input-single-output (SISO) filter for each polarization and polarization demultiplexing with a single-tap 2×2 SL filter on both sides of SISO filters. Constraining SISO filters to compensate for the delay only, polarization demultiplexing without excessive compensation can be achieved.

The signal processing flow is as follows. The adaptive ML filters without delay constraints are performed and calculate d_x and d_y from SISO filter coefficients. Then, the adaptive ML filters with delay constraints are performed again. The obtained filter coefficients of 2×1 SL filters and

2×1 WL filters are converted to 2×2 real-valued IQ multi-input-multi-output (MIMO) filter coefficients h_{II} , h_{QI} , h_{IQ} , and h_{QQ} for each polarization [10], which is used for fixed Tx and Rx compensation by FDE in the main DSP.

Since ML filters rely on standard coherent transceiver hardware, no dedicated hardware is required. Further, it can be offloaded from the main DSP as transceiver distortion proceeds slowly. The proposed calibration allows the main DSP to minimize the number of taps for 2×2 SL filter since Tx/Rx FDE compensates IQ common distortion in Tx and Rx devices, respectively.

Experimental setup and offline DSP

Fig. 3 shows the experimental setup and offline DSP for 96-Gbaud-root raised cosine filtering (RRC)-PM-64QAM transmission. The roll-off factor of 0.01 was used. External cavity lasers (ECL) with a 100 kHz linewidth were used for both signal source and local oscillator (LO). On the Tx side, the electrical signal was modulated with a coherent driver modulator (CDM) class 60 [15], including driver amplifiers and PM-IQ modulator, and four 120-GSa/s DAC. Random bits were loaded to the payload and mapped to PM-64QAM. Different seeds were used to generate random bits for calibration and signal evaluation with the main DSP. A pilot sequence was inserted for each polarization to perform a pilot-based DSP [16]. One pilot symbol of QPSK was inserted every 25 symbols with 2^{10} QPSK overhead for filter pre-convergence, a total of 91175 symbols. IQ skew and gain imbalance in Tx/Rx were pre-adjusted to focus on the frequency-dependent transceiver distortion. We used 120 km SMF for the transmission line with 100 rad/s polarization scrambling. The fibre launch power was set to 0 dBm where the fibre nonlinearity is negligible to verify Tx nonlinearly effect of the calibration, resulting in a received OSNR of 32.6 dB/0.1nm. After optical bandpass filtering (OBPF), the optical signal was received

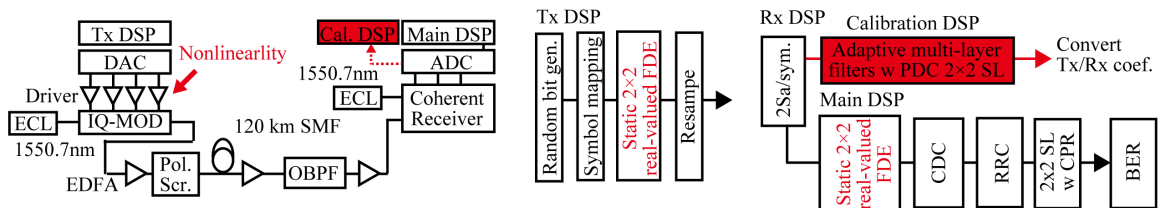


Fig. 3: Experimental setup and offline DSP

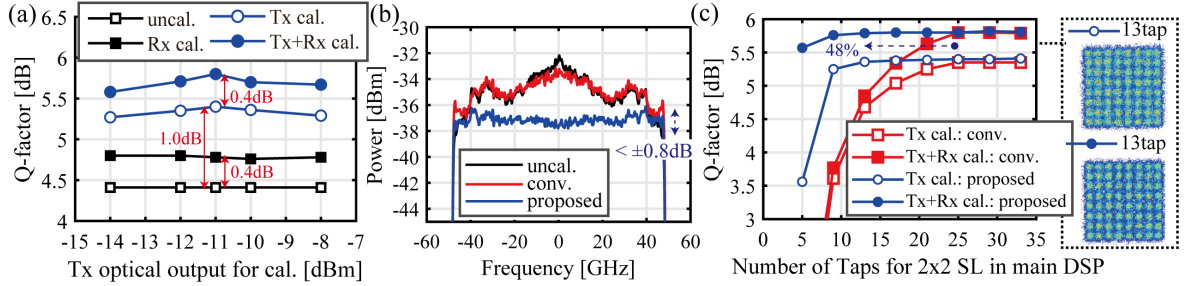


Fig. 4: Experimental results (a) Q-factor as a function of Tx optical output for calibration, (b) Tx optical spectrum (res.:500MHz), (c) Q-factor as a function of number of taps for 2×2 SL filter in the main DSP

coherently and digitalized with four 256-GSa/s analog-to-digital converter (ADC).

The validation consists of calibrating by deriving the Tx and Rx FDE filter coefficients and then by signal evaluation by the main DSP using Tx/Rx FDE-based compensation with calibrated coefficient. For the calibration, 2-Sa/sym. signal was fed to the proposed adaptive ML filters. Tx nonlinearity in CDM was induced by tuning DAC outputs. 201 tap was selected to compensate for the frequency response of Tx/Rx devices, and 53 taps was set for SISO filters to compensate for delays precisely. The filter coefficient update was carried out using the known transmit symbol with data-aided least-mean-square (DA-LMS). The conventional ML filter-based calibration was also performed for comparison; 25 tap was set for the conventional 2×2 SL filter, and DAC output was adjusted to the linear region. The obtained 2×2 real-valued MIMO filter coefficients were set Tx and Rx FDE, respectively.

In the main DSP, Tx and Rx FDE-based compensation was applied. Tx power was set to -11 dBm for all verification. In the main Rx DSP, CD was compensated after Rx FDE. Matched RRC filtering was applied to the output of CDC. T/2-spaced phase-lock-loop (PLL) based 2×2 SL filter with 25 taps was performed with CPR. The filter coefficient was updated using the pilot symbol with DA-LMS. After demodulation, Q-factor was calculated from the bit error rate (BER).

Results and Discussion

First, we evaluated the nonlinearity effect in the proposed scheme. In Fig. 4 (a), Q-factor was plotted as a function of Tx optical output for calibration. The uncalibrated case was used as a benchmark, and Q-factor was averaged over two polarization signals. Overall, Q-factor was improved with the proposed calibration. With Rx calibration, Q-factor was almost constant, improving the Q-factor by 0.4 dB from the uncalibrated case. With Tx calibration, Q improvement varied slightly with Tx output, -11 dBm for calibration gave the best results in this study, and Q-improvement was 1.0 dB. Both Tx/Rx calibration improved Q-factor by 1.4 dB,

indicating that the calibration was working for both Tx and Rx, respectively.

Next, we compared the proposed calibration for the calibration without PDC. Tx optical signal spectrums are shown in Fig. 4 (b). It is observed that the frequency response was not fully compensated for the calibration without PDC; only small gain equalization was achieved within ± 1.9 dB ripple. In contrast, the proposed calibration showed a flat frequency response within ± 0.8 dB ripple, indicating successful separation of Tx and Rx compensations.

In Fig. 4 (c), Q-factors are plotted as a function of the number of taps for 2×2 SL filter in the main DSP. The calibration without PDC required 25 taps to achieve a saturated Q-factor for both Tx and Tx/Rx calibration cases. We assume that 2×2 SL filter corrected most IQ common distortions during the calibration. Meanwhile, the proposed method did not degrade when the taps were reduced by 48% to 13 taps in either case, as the proposed calibration compensated IQ common distortions by Tx and Rx filter. It shows that the number of taps for 2×2 SL filter in the main DSP can be minimized for transmission impairment only while ensuring performance by the proposed on-site calibration.

Conclusions

We have proposed on-site transceiver calibration using adaptive multi-layer filters with PDC and weak Tx nonlinearity aid, realizing Tx-Rx separation. Our method was demonstrated with 96-Gbaud PM-64QAM 120km transmission experiment, which effectively separated Tx/Rx distortion and compensation of IQ common distortion; we showed flat Tx frequency response within ± 0.8 dB ripple and 48 % reduction of 2×2 SL filter tap in the main DSP, compared to the conventional calibration.

Acknowledgements

Part of these research results was obtained within “The research and development of advanced optical transmission technology for a green society” (JPMI00316) of the Ministry of Internal Affairs and Communications, Japan.

References

- [1] P. J. Winzer, D. T. Neilson, and A. R. Chraplyvy, "Fiber-optic transmission and networking: the previous 20 and the next 20 years", *Opt. Express*, vol. 26, no. 18, pp. 24190–24239, 2018. DOI: [10.1364/OE.26.024190](https://doi.org/10.1364/OE.26.024190)
- [2] A. Matsushita, M. Nakamura, F. Hamaoka, S. Okamoto, and Y. Kisaka, "High-Spectral-Efficiency 600-Gbps/Carrier Transmission Using PDM-256QAM Format", *J. Lightw. Technol.*, vol. 30, no. 7, pp. 470–476, 2019. DOI: [10.1109/JLT.2018.2890124](https://doi.org/10.1109/JLT.2018.2890124)
- [3] X. Chen and D. Che, "Direct-Detection Based Frequency-Resolved I/Q Imbalance Calibration for Coherent Optical Transmitters", OFC, San Francisco, USA, 2021, Th5D.3. DOI: [10.1364/OFC.2021.Th5D.3](https://doi.org/10.1364/OFC.2021.Th5D.3)
- [4] Y. Yoshida, S. Yoshida, S. Oda, T. Hoshida, and N. Yamamoto, "Simultaneous Monitoring of Frequency-dependent IQ Imbalance in a Dual-polarization IQ Modulator by using a Single Photodetector: A Phase Retrieval Approach", OFC, San Francisco, USA, 2021, Th5D.2. DOI: [10.1364/OFC.2021.Th5D.2](https://doi.org/10.1364/OFC.2021.Th5D.2)
- [5] H. Ji, Y. Yang, Z. Xu, Z. He, W. Hu, and W. Shieh, "Single-shot Characterization of Frequency-resolved Imbalance in Coherent Transceivers Based on Inter-channel Response Ratio", *J. Lightw. Technol.*, Early Access, 2023. DOI: [10.1109/JLT.2023.3259463](https://doi.org/10.1109/JLT.2023.3259463)
- [6] C. Fludger and T. Kupfer, "Transmitter Impairment Mitigation and Monitoring for High Baud-Rate, High Order Modulation Systems", ECOC, Düsseldorf, Germany, 2016, Tu 2.A.2.
- [7] M. Sato, M. Arikawa, H. Noguchi, J. Matsui, J. Abe, and E. L. T. de Gabory, "Mitigation of Transmitter Impairment with 4×2 WL MIMO Equalizer Embedding Preliminary CPR", OFC, San Diego, USA, 2022, M1H.5. DOI: [10.1364/OFC.2022.M1H.5](https://doi.org/10.1364/OFC.2022.M1H.5)
- [8] R. Rios-Müller and J. Renaudier, "Blind receiver skew compensation and estimation for long-haul non-dispersion managed systems using adaptive equalizer", *J. Lightw. Technol.*, vol. 33, no. 7, pp. 1315–1318, 2015. DOI: [10.1109/JLT.2014.2377582](https://doi.org/10.1109/JLT.2014.2377582)
- [9] M. Arikawa and K. Hayashi, "Adaptive equalization of transmitter and receiver IQ skew by multi-layer linear and widely linear filters with deep unfolding", *Opt. Express*, vol. 28, no. 16, pp. 23478–23494, 2020. DOI: [10.1364/OE.395361](https://doi.org/10.1364/OE.395361)
- [10] M. Arikawa and K. Hayashi, "Transmitter and receiver impairment monitoring using adaptive multi-layer linear and widely linear filter coefficients controlled by stochastic gradient descent", *Opt. Express*, vol. 29, no. 8, pp. 11548–11561, 2021. DOI: [10.1364/OE.416992](https://doi.org/10.1364/OE.416992)
- [11] M. Arikawa, M. Sato, and K. Hayashi, "Compensation and monitoring of transmitter and receiver impairments in 10,000-km single-mode fiber transmission by adaptive multi-layer filters with augmented inputs", *Opt. Express*, vol. 30, no. 12, pp. 20333–20359, 2022. DOI: [10.1364/OE.459959](https://doi.org/10.1364/OE.459959)
- [12] T. Kobayashi, M. Nakamura, F. Hamaoka, M. Nagatani, H. Wakita, H. Yamazaki, T. Umeki, H. Nosaka, and Y. Miyamoto, "35-Tb/s C-band Transmission over 800 km Employing 1-Tb/s PS-64QAM signals enhanced by Complex 8 × 2 MIMO Equalizer", OFC, San Diego, USA, 2019, Th4B.2. DOI: [10.1364/OFC.2019.Th4B.2](https://doi.org/10.1364/OFC.2019.Th4B.2)
- [13] A. Kawai, M. Nakamura, T. Kobayashi, and Y. Miyamoto, "Digital Four-Dimensional Transceiver IQ Characterization", *J. Lightw. Technol.*, vol. 41, no. 5, pp. 1389–1398, 2023. DOI: [10.1109/JLT.2022.3224916](https://doi.org/10.1109/JLT.2022.3224916)
- [14] R. M. Büttler, C. Häger, H. D. Pfister, G. Liga, and A. Alvarado, "Model-Based Machine Learning for Joint Digital Backpropagation and PMD Compensation", *J. Lightw. Technol.*, vol. 39, no. 4, pp. 949–959, 2021. DOI: [10.1109/JLT.2020.3034047](https://doi.org/10.1109/JLT.2020.3034047)
- [15] OIF-HB-CDM-02.0 – Implementation Agreement for High Bandwidth Coherent Driver Modulator (2021). <https://www.oiforum.com/wp-content/uploads/OIF-HB-CDM-02.0.pdf>
- [16] M. Mazur et al., "Overhead-optimization of pilot-based digital signal processing for flexible high spectral efficiency transmission", *Opt. Express*, vol. 27, no. 17, pp. 24654–24669, 2019. DOI: doi.org/10.1364/OE.27.024654